Naval Research Laboratory

Washington, DC 20375-5320

NRL/MR/5750--17-9747

Application of Statistical Linear Time-Varying System Theory to Modeling of High Grazing Angle Sea Clutter

Donald E. Jarvis

Advanced Techniques Branch
Tactical Electronic Warfare Division

Corey D. Cooke

Applied Technology, Inc.
King George, Virginia

October 25, 2017

REPORT DOCUMENTATION PAGE

Form Approved
OMB No. 0704-0188

1. REPORT DATE *(DD-MM-YYYY)*
25-10-2017

2. REPORT TYPE
NRL Memorandum Report

3. DATES COVERED *(From - To)*
January 2017 – May 2017

4. TITLE AND SUBTITLE
Application of Statistical Linear Time-Varying System Theory to Modeling of High Grazing Angle Sea Clutter

5a. CONTRACT NUMBER
N00173-17-D-2003/N0024-5-C-5346

5b. GRANT NUMBER

5c. PROGRAM ELEMENT NUMBER
NFE 2007-004

6. AUTHOR(S)
Donald E. Jarvis and Corey D. Cooke*

5d. PROJECT NUMBER

5e. TASK NUMBER
N00173-17-F-2010

5f. WORK UNIT NUMBER

7. PERFORMING ORGANIZATION NAME(S) AND ADDRESS(ES)
Naval Research Laboratory
4555 Overlook Avenue, SW
Washington, DC 20375-5320

8. PERFORMING ORGANIZATION REPORT NUMBER
NRL/MR/5750--17-9747

9. SPONSORING / MONITORING AGENCY NAME(S) AND ADDRESS(ES)
Raytheon Company
1847 West Main Road
Portsmouth, RI 02871

Naval Sea Systems Command
1333 Isaac Hull Avenue SE
Washington Navy Yard, DC 20376

10. SPONSOR / MONITOR'S ACRONYM(S)
RTN/NAVSEA

11. SPONSOR / MONITOR'S REPORT NUMBER(S)

12. DISTRIBUTION / AVAILABILITY STATEMENT
Approved for public release; distribution is unlimited.

13. SUPPLEMENTARY NOTES
*Applied Technology, Inc., 5200 Potomac Dr., King George, VA, 22485

14. ABSTRACT
Historically, radar returns from the sea surface have generally been modeled one of two ways--either (a) a quasi-deterministic fashion using electromagnetic scattering theory combined with a random realization of physical sea surface based on insights from hydrodynamics or (b) using a primarily statistical formulation of the amplitude envelope using assumptions about the distribution of scatterers within a resolution cell based on vague physical insights. However, these models suffer from excessive computational and/or conceptual complexity or have highly restrictive regimes of applicability. In this work, we present an alternative characterization of sea clutter returns utilizing statistical linear time-varying system theory in an attempt to provide a more general model that works in a wider variety of circumstances while retaining a competitively low computational burden. It is hoped that the compactness of this mathematical representation will facilitate more rapid development of effective clutter mitigation techniques in the future.

15. SUBJECT TERMS
Time-frequency analysis
Linear time-varying systems
Sea clutter modeling

16. SECURITY CLASSIFICATION OF: a. REPORT	b. ABSTRACT	c. THIS PAGE	17. LIMITATION OF ABSTRACT	18. NUMBER OF PAGES	19a. NAME OF RESPONSIBLE PERSON
Unclassified Unlimited	Unclassified Unlimited	Unclassified Unlimited	SAR Unlimited	28	Corey D. Cooke
					19b. TELEPHONE NUMBER *(include area code)* 202-767-6351

Standard Form 298 (Rev. 8-98)
Prescribed by ANSI Std. Z39.18

CONTENTS

EXECUTIVE SUMMARY E-1

1. INTRODUCTION 1
   1.1 Proposed Approach 1
   1.2 Literature Survey 2

2. MATHEMATICAL BACKGROUND 2
   2.1 Simulation Geometry 4
   2.2 Wide-Sense Stationary/Uncorrelated Scattering (WSSUS) Linear Time-Varying (LTV) System Theory 5

3. WSSUS SEA CLUTTER SCATTERING FUNCTION 9
   3.1 Delay-Doppler Derivation 9
   3.2 Time-Frequency Power Distribution at Channel Output 16
   3.3 Signal-to-Clutter Ratio 19

4. CONCLUSION AND FUTURE WORK 20

ACKNOWLEDGMENTS 20

REFERENCES 21

FIGURES

1 Example swell wave process realization generated from a narrow-band gravity wave spectrum from [33]. 3

2 Flat earth geometry in the $x - z$ plane. 3

3 Illustration of sequential returns from isorange rings on the sea surface. 4

4 Differential area of isorange ring at ground range g. 6

5 Clutter patch returns for a single isorange ring. 10

6 Normalized Doppler spectrum for an isotropic radiator with $v_z = 0$. 13

7 Normalized Doppler spectrum for a directive radiator with $v_z = 0$. 13

8 Scattering function of sea clutter channel. 15

9 Ambiguity function for a train of unmodulated rectangular pulses. 17

10 Output power distribution from a sea clutter channel with an input pulse train of unmodulated rectangular pulses. 18

EXECUTIVE SUMMARY

Sea clutter mitigation is an essential feature of airborne radars operating in a maritime environment because the radar return from the sea surface can easily obscure targets of interest, therefore being able to accurately model the sea clutter returns is an essential step in the design process.

Much work has been done in the area of sea clutter modeling, including measurement campaigns, statistical characterization, and electromagnetic (EM) scattering computations. However, these models are usually purpose-built to solve a specific problem and are rarely general in character. A more comprehensive statistical characterization is also desired that does not impose a large computational burden like an EM scattering computation would.

In this work we present a general framework for modeling sea clutter returns from a signal processing perspective by modeling the sea clutter scattering channel as a random linear time-varying system. Linear time-varying system theory has been studied rigorously since the 1960's, and by casting the clutter scattering problem in this form, we can apply standard analytical tools immediately to gain new insight into the time-frequency characteristics of clutter returns.

The mathematical formulation of sea clutter in this work is hoped to provide a unifying structure that will enhance the future development of clutter mitigation techniques, particularly in the design of radar waveforms and signal processing techniques.

APPLICATION OF STATISTICAL LINEAR TIME-VARYING SYSTEM THEORY TO MODELING OF HIGH GRAZING ANGLE SEA CLUTTER

1. INTRODUCTION

1.1 Proposed Approach

Another approach to modeling clutter which has not received much attention in the literature is to use tools from linear time-varying system theory. A linear time-varying (LTV) system is one whose properties change with time. In the case of a linear time-invariant (LTI) system the output signal $y(t)$ can be expressed using the convolution of the input signal $x(t)$ with the impulse response $h(t)$:

$$y(t) = \int h(\tau)x(t-\tau)d\tau. \tag{1}$$

In this case, $y(t)$ can be seen as the superposition of copies of $x(t)$, each delayed by a lag τ and scaled by a coefficient $h(\tau)$. In an LTV system, the impulse response depends on both t and τ [1] and thus the scaling coefficient now changes with time and becomes $h(\tau, t)$:

$$y(t) = \int h(\tau, t)x(t-\tau)d\tau. \tag{2}$$

Due to the fact that the LTV approach is very prevalent in wireless communication theory in modeling multipath fading channels, it is common to refer to the system represented by h as the "channel". Changes in h with t characterize changes in the channel over time, e.g. if a scatterer is moving, which can introduce Doppler frequency shifts in the received signal. (In this work we assume the velocities involved are small relative to the speed of light and thus that the Doppler effect affects only the carrier frequency and not the time-scaling of the signal envelope.)

Because of the multitude of small variations on the sea surface and the impracticality of modeling the exact sea surface at a specified point on the earth, we will model the radar reflection off the sea surface as a random linear time-varying system. The fundamental work on random LTV system theory was performed by Bello [2] where he introduces the concept of a wide-sense stationary uncorrelated scattering (WSSUS) channel.

LTV system theory has been primarily used by wireless communications researchers [1, 3, 4] for designing adaptive radios that adjust their modulations based on changing channel parameters, such as the channel coherence time and coherence bandwidth, which describe properties of $h(\tau, t)$. However, one of the initial uses of random LTV system theory was in describing distributed radar returns from a large object (such as a planet) in radio astronomy as a function of delay and Doppler shift using a so-called "scattering

Manuscript approved July 14, 2017.

function" [5, 6]. The use of scattering functions for modeling radar returns are also described by Van Trees in his seminal book series [7], by Kay in at least one paper [8], and are mentioned by a small number of other authors (e.g. [9–15]), but in general are not commonly referred to in the radar literature or used widely among practicing radar engineers.

In this work we propose the use of LTV system theory for modeling sea clutter returns so that these tools from decades of research can be applied to accurately characterize the time-frequency characteristics of sea clutter to enhance the development of more effective clutter mitigation techniques, particularly in the area of waveform design [16, 17]. This approach attempts to capture enough of the essential signal characteristics to be useful while retaining the low computational burden of the statistical models from which it is built on.

1.2 Literature Survey

Like many early developments in RF/microwave technology, the first systematic presentation of research on sea clutter was published in a MIT Radiation Laboratory series book chapter by Kerr and Goldstein [18]. In this work, the concept of a normalized radar cross-section (NRCS), σ^0, is introduced along with a rather comprehensive description of sea clutter generation mechanisms as they were understood at the time. Other early research discusses the dependence of the NRCS on frequency, grazing angle, and wind speeds [19, 20]. Other early work studied the scattering from rough and periodic structures on the sea surface [21, 22]. A good summary overview of the work of these early decades is given by Barton [23]. Much work focuses on the unique characteristics of clutter as seen from low grazing angles [24].

Sea clutter modeling techniques generally fall into one of two main categories– statistical approaches and quasi-deterministic electromagnetic approaches. (Granted, most methods are not exclusively one or the other, but rather, we are assigning them to the group with which their approach most closely aligns.)

Statistical models model the sea clutter return as a stochastic process whose magnitude return follows a specified distribution. Rayleigh clutter is considered the simplest case, arising from central limit theorem arguments when the number of scatterers in a resolution cell is sufficiently large [25]. However, when the radar resolution increases and particularly when the grazing angle is less than $10°$ (which is a common definition for "low grazing angle"), individual wave "spikes" become resolvable and the distribution becomes more heavy-tailed. While a number of distributions have been proposed to model low-grazing angle clutter, one of the most prominent was the K-distribution, first proposed by Jakeman and Pusey [26–29] and promoted by Ward, Tough, and Watts [25, 30–32]. Statistical methods have the advantage that they are relatively computationally inexpensive.

Quasi-deterministic approaches generally begin by creating a random sea surface generated from a specified wave spectrum, such as is shown in Figure 1 from which a deterministic electromagnetic scattering computation is performed [33]. Ott gives a good overview and comparison of many such models, including the well-known TEMPER and VTRPE models [34]. While these methods may more accurately model the fundamental physics of the problem, they generally impose a much more severe computational burden on any sea clutter simulation, which is a severe disadvantage.

2. MATHEMATICAL BACKGROUND

In this section we will derive statistical characterizations of the impulse response of the sea clutter scattering channel by modeling it as a zero-mean WSSUS random process.

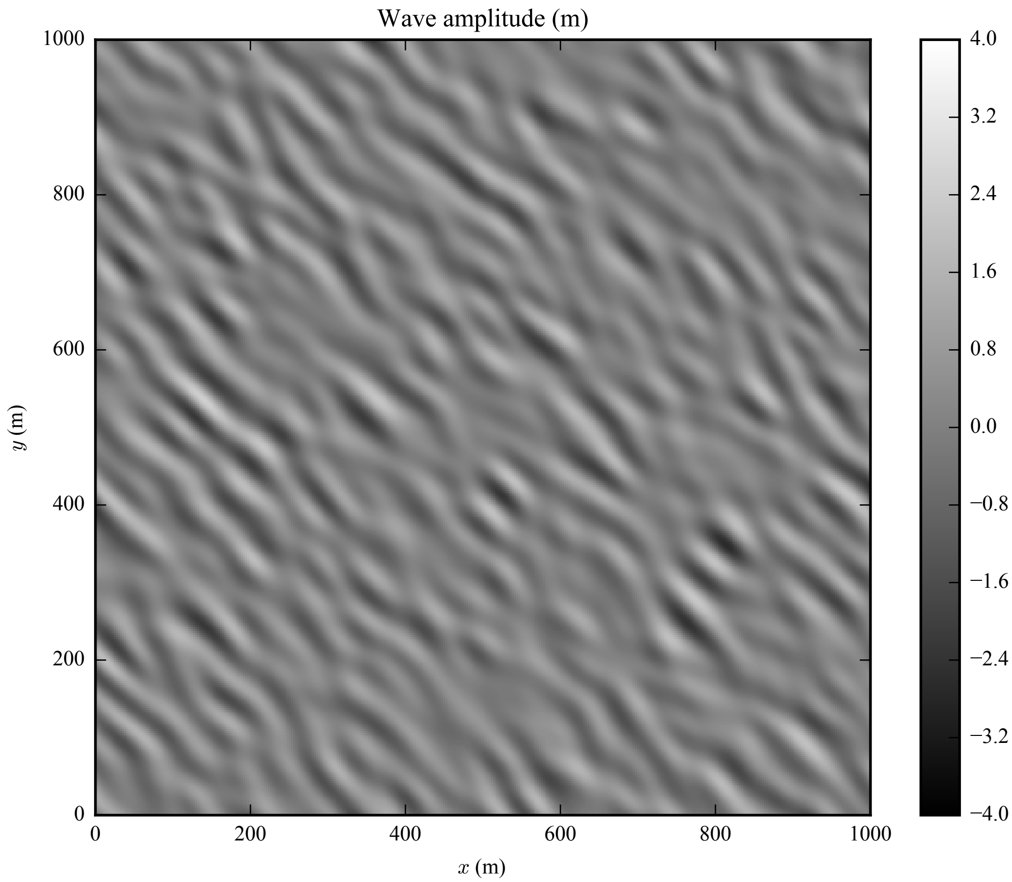

Fig. 1: Example swell wave process realization generated from a narrow-band gravity wave spectrum from [33].

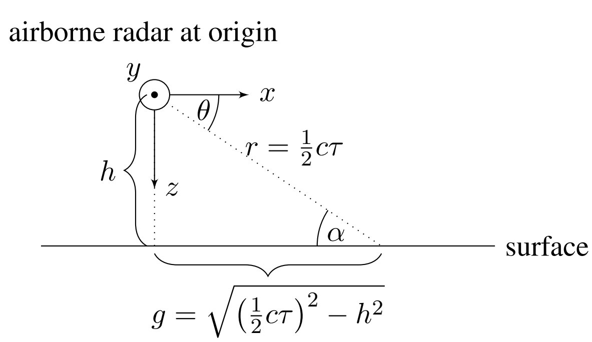

Fig. 2: Flat earth geometry in the $x - z$ plane.

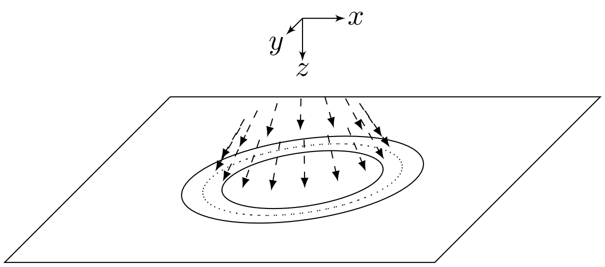

(a) Transmitted signal to isorange ring at ground range g.

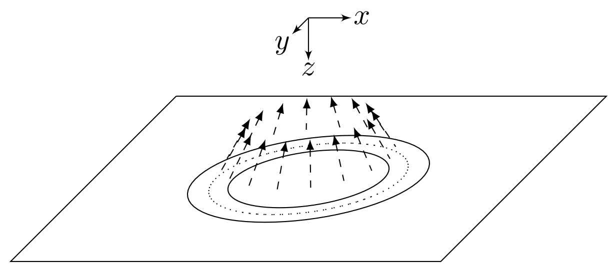

(b) Reflected signal from isorange ring at ground range g.

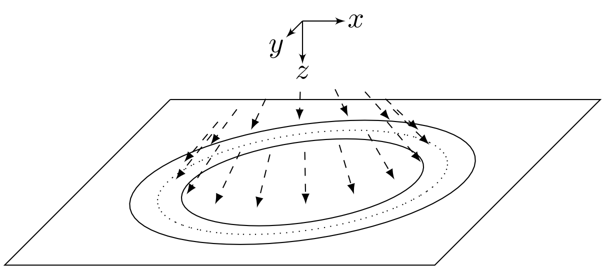

(c) Transmitted signal to the next isorange ring, at ground range $g + dg$.

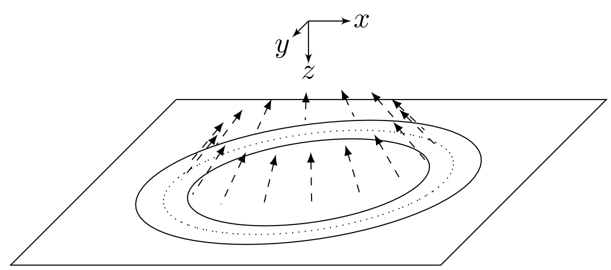

(d) Reflected signal from the next isorange ring, at ground range $g + dg$.

Fig. 3: Illustration of sequential returns from isorange rings on the sea surface.

2.1 Simulation Geometry

First we must define the simulation geometry. We will assume that the radar of interest being modeled is in an airborne platform with altitude h above the sea surface, as shown in Figure 2. In this figure the variables r, g, and h represent slant range, ground range, and altitude, respectively, and θ and α represent the depression and grazing angles, respectively. For a flat earth geometry, $\alpha = \theta$. The coordinate axes are oriented such that the platform is located at the origin and the $x - z$ plane is oriented such that the platform velocity vector $\mathbf{v} = [v_x, v_y, v_z]^T$ always lies in the $x - z$ plane. (This implies that $v_y = 0$.) Because we are seeking to model the channel characteristics as a function of t and τ, we will express all geometric quantities in terms of these variables. (The picture in Figure 2 is given for a fixed value of t– we will account for the platform velocity at a later point.) Thus, the range r is given as $r = \frac{1}{2}c\tau$ and g is solved for using the Pythagorean theorem:

$$g = \sqrt{\left(\frac{1}{2}c\tau\right)^2 - h^2}, \tag{3}$$

where c is the speed of light and h is assumed fixed.

We will model the radar signal as a spherical wave emanating from the source located at the origin as is shown in Figure 3. Each small segment of the wave reflects successively off isorange rings on the sea surface; the total return is therefore the summation of the returns from each isorange ring.

The power gain as a function of delay can be obtained using the radar range equation [35]:

$$\frac{P_R}{P_T} = \frac{G^2(\phi(\tau), \theta(\tau))\, \lambda^2\, \sigma^0(\alpha(\tau))\, dA(\tau)}{(4\pi)^3\, (\frac{1}{2}c\tau)^4} \tag{4}$$

where

- P_T = transmitted power (average power during pulse duration)
- P_R = receive power
- ϕ, θ = azimuth and depression angles, respectively, such that:

  $$x = r\cos\theta\cos\phi$$
  $$y = r\cos\theta\sin\phi$$
  $$z = r\sin\theta$$

- α = grazing angle, which for a flat earth model is $\alpha = \theta = \sin^{-1}(h/(\frac{1}{2}c\tau))$
- $G(\phi, \theta)$ = antenna power gain as a function of look direction
- λ = wavelength = c/f
- $\sigma^0(\alpha)$ = normalized RCS (NRCS) of sea surface as a function of grazing angle α for some fixed wavelength and sea state
- $dA(\tau)$ = differential surface area of isorange ring at delay τ.

The differential surface area dA computation (assuming a flat earth model) is illustrated in Figure 4 and is derived as follows:

$$\begin{aligned} dA = g\, dg\, d\phi = (g) \cdot \left(\frac{dg}{d\tau}\, d\tau\right) \cdot (2\pi) &= \left(\sqrt{\left(\frac{1}{2}c\tau\right)^2 - h^2}\right) \cdot \left(\frac{c^2\tau}{4\sqrt{\left(\frac{1}{2}c\tau\right)^2 - h^2}}\, d\tau\right) \cdot (2\pi) \\ &= \frac{\pi}{2}c^2\tau\, d\tau \qquad (5) \\ \implies \frac{dA}{d\tau} &= \frac{\pi}{2}c^2\tau \qquad (6) \end{aligned}$$

2.2 Wide-Sense Stationary/Uncorrelated Scattering (WSSUS) Linear Time-Varying (LTV) System Theory

2.2.1 Overview and fundamental definitions

The theory of random WSSUS LTV systems was first illustrated by Bello in his landmark paper [2] and his approach has been used successfully for decades in the wireless communication community to model signal amplitude fluctuations in mobile radio. (The mobility of the radio nodes creates changing

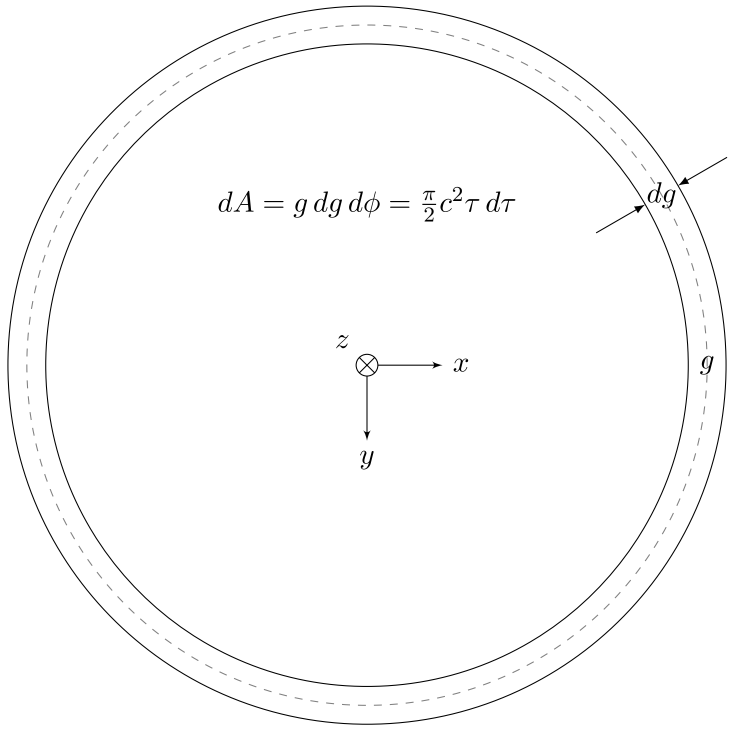

Fig. 4: Differential area of isorange ring at ground range g.

geometry of the wireless channel and makes the channel impulse response appear random.) Because an LTV system implicitly models motion, LTV system theory is well-suited to modeling the Doppler effect of moving scatterers, such as is present in a radar system. In fact, the only substantial differences between the communications application versus the radar application from a linear systems perspective is that in a radar the transmitter and receiver are co-located, and in a radar system the antenna is generally highly directive, whereas in mobile radio the antenna is usually assumed to be omnidirectional [1]. (In the case of a single-antenna system this is true; newer multiple input-multiple output (MIMO) radio systems with multiple antennas at both the base station and mobile node violate this assumption.)

To apply the WSSUS assumption to a radar scattering channel, we will express the impulse response in the following form:

$$h(\tau, t) = \int_{-\infty}^{\infty} \eta(\tau, \rho)\, e^{j2\pi\rho t}\, d\rho \tag{7}$$

where ρ is the Doppler shift and $\eta(\tau, \rho)$ is known as the "delay-doppler spread function" [10, 15]. This function describes the scattering amplitude at a given delay (range) and Doppler shift. Substituting (7) into (2) yields:

$$y(t) = \int_{-\infty}^{\infty}\int_{-\infty}^{\infty} \eta(\tau, \rho)\, x(t-\tau)\, e^{j2\pi\rho t}\, d\rho\, d\tau, \tag{8}$$

where $x(t)$ is the transmitted signal (at baseband) and $y(t)$ is the received signal. In (8) it is clear to see that y(t) can be expressed as the superposition of delayed (by τ), frequency-shifted (by ρ), and scaled (by the complex gain $\eta(\tau, \rho)$) copies of $x(t)$. It should be noted that this definition is general enough to include *all* scatterers in the radar's field of view– clutter as well as useful targets. In this case the overall delay-Doppler spreading function is:

$$\eta_{\text{total}} = \eta_{\text{targets}} + \eta_{\text{clutter}} \tag{9}$$

due to the linearity of the system.

In the case of sea clutter, the multitude of minute variations of the sea surface make it appear extremely random, and thus we will assume that η and h are in general a stochastic process in this work. To characterize the behavior of sea clutter we will assume that it is zero-mean and compute its second-order statistics:

$$R_h(\tau, \tau', t, t + \Delta t) = \mathbb{E}\left[h^*(\tau, t)\, h(\tau', t + \Delta t)\right] \tag{10}$$

Here we apply two fundamental assumptions: 1) The signal is wide-sense stationary (WSS), implying that the autocorrelation depends only on Δt on the time axis, and 2) the scattering at different lags τ is uncorrelated:

$$\begin{aligned} \mathbb{E}\left[h^*(\tau, t)\, h(\tau', t + \Delta t)\right] &= R_h(\tau, \tau', \Delta t) \\ &= A_h(\tau, \Delta t)\, \delta(\tau - \tau') \end{aligned} \tag{11}$$

The function $A_h(\tau, \Delta t)$ is known as the channel correlation function, and describes the distribution of the radar return as a function of lag τ and correlation time Δt [1, 3].

In an airborne pulse-Doppler radar system we can think of the channel as being roughly constant during a single pulse duration, but that the channel changes slightly between pulses (e.g. a small phase rotation due to the Doppler offset of the return). Under this view, we can treat the variable τ as the downrange delay (or the "fast time" in a radar data cube [17]) and the variable Δt as capturing the evolution of the channel over "slow time". By taking the Fourier transform of $A_h(\tau, \Delta t)$ with respect to Δt, we can view the Doppler spectrum of the return as a function of delay. The so-called "scattering function" is defined as follows:

$$C_\eta(\tau, \rho) = \mathcal{F}_{\Delta t}\left[A_h(\tau, \Delta t)\right] = \int_{-\infty}^{\infty} A_h(\tau, \Delta t) e^{-j2\pi\rho\Delta t} d\Delta t. \tag{12}$$

The scattering function provides a measure of the output channel power as a function of delay and Doppler. It was first introduced formally by Price and Green [5, 6] but was first hinted at in a paper by Westerfield [36]. This function played a prominent role in Bello's fundamental paper where he coined the WSSUS nomenclature and showed the two-dimensional Fourier transform relationships (i.e. along the $\Delta t \leftrightarrow \rho$ dimension and along the $\tau \leftrightarrow \Delta f$ dimension) between four related functions that equally capture the time-frequency characteristics of a WSSUS channel, two of which we have described here ($A_h(\tau, \Delta t)$ and $C_\eta(\tau, \rho)$). As was mentioned earlier, the scattering function has been used to characterize radar returns since its formal inception by Price and Green, who used it to model returns from large distributed targets such as the return from a planet in radar astronomy. Van Trees also briefly describes the scattering function in his

most well-known book [7], as does Kay in at least one paper [8], but despite the prestige associated with some of its proponents, it has remained a niche mathematical tool that sees little practical use. It is uncertain why this is the case, given the relative simplicity it allows one to describe a radar scattering channel.

It can also be shown that the autocorrelation function of the delay-doppler spread function η for a WSSUS channel is:

$$\mathbb{E}\left[\eta^*(\tau,\rho)\,\eta(\tau',\rho')\right] = C_\eta(\tau,\rho)\,\delta(\tau-\tau')\,\delta(\rho-\rho'). \tag{13}$$

(It is sometimes easier to work with this form when deriving new expressions.)

Note that nowhere in this discussion have we yet specified a distribution for the samples of $h(\tau,t)$. If we take the further step of specifying that h is a complex Gaussian random process with independent real and imaginary components, then the distribution of h is completely specified by either the correlation function A_h or the scattering function C_η, and sample realizations of h can be generated by filtering white noise to have the Doppler spectrum determined by C_η. It is well known that when the values of h are given by a complex Gaussian, the magnitude envelope $|h|$ will be Rayleigh-distributed and the power $|h|^2$ will be exponentially distributed [1]. The Rayleigh distribution was the de-facto standard for modeling sea clutter returns for early radars and is a good approximation when the beam footprint (and range resolution) is wide and/or the grazing angle is large and thus encompasses a large number of independent scatterers whose returns are assumed to sum to be approximately Gaussian using central limit theorem arguments [25, 37].

2.2.2 *Validity of the WSSUS assumption*

We have assumed that the channel is both wide-sense stationary (WSS) (statistics depend only on Δt, not t) and that there is uncorrelated scattering (US) (i.e. the returns are uncorrelated for different values of τ). The WSS assumption is relatively noncontroversial– over the course of a single CPI, which is on the order of milliseconds, or even several CPIs, it seems very reasonable that the physical state of the sea will have not changed significantly. (This is equivalent to saying that the joint probability density of the sea surface properties retain the same statistics over this time period.) The US assumption, however, is much more controversial, due to the fact that the dimensions of larger sea surface features (such as swell waves) are much larger than the radar resolution, implying that there will be correlation between the returns in closely-spaced range bins [25].

One way of introducing correlation in the τ dimension would be to replace the delta function in (11) with a function such as a decaying exponential to express correlation between adjacent range samples:

$$R_h(\tau,\tau',\Delta t) = A_h(\tau,\Delta t)e^{-|\tau-\tau'|/T_c}, \tag{14}$$

where T_c is a correlation length, usually determined empirically. Many models exist for modeling spatial correlation of sea clutter [38]; one formula for correlation length (in meters) is given by [24]:

$$r_c = \frac{\pi}{2}\frac{U^2}{g}\sqrt{3\cos^2\phi_w + 1} = \frac{1}{2}cT_c \tag{15}$$

where U is the wind speed in m/s, $g \approx 9.81$ m/s is the gravitational constant, and ϕ_w is the wind direction. For example, if the wind speed is 10 m/s (corresponding approximately to Douglas sea state 4 or "rough sea" [25]), the maximum correlation length is 32.02 m or approximately 213.6 ns of lag. If this distance is greater than the range resolution of the radar operating in that environment, then it cannot be assumed that the clutter return is white and matched filter-based detectors will perform sub-optimally [17]. In other words, estimates of the signal-to-clutter ratio based on the WSSUS assumption will be too optimistic if significant range correlation exists. One way of modeling the spatial correlation of clutter would be to generate WSSUS clutter samples then filter them along the τ axis with a filter designed using (15) whose spectral characteristics approximate that of the clutter spectrum.

Non-WSSUS LTV systems have been studied by some authors (e.g. [39]), but for simplicity's sake we will use the WSSUS model in this work so we can produce an elementary result to fill the immediate need for a first-order model to develop further intuition of sea clutter scattering channels and leave the non-WSSUS formulation to future work.

3. WSSUS SEA CLUTTER SCATTERING FUNCTION

To create a model for $C_\eta(\tau, \rho)$, we need to characterize the signal return in range (via τ) and Doppler (via ρ). The majority of the decay in signal amplitude with τ we have already accounted for in (4). To account for the Doppler characteristics we will consider the return from a single isorange ring and then later combine our results into a single function.

3.1 Delay-Doppler Derivation

Using the Clarke model for uniform scattering [40, 41] that is widely used in the wireless communication field as a guide, we will derive Doppler spectrum of the scattered sea clutter signal at a single small isorange ring located at ground range g with width dg.

We will assume that the impulse response from this ring is a sum of N delta functions with a time-varying amplitude and phase (which encompasses the Doppler shift as well). We will segment the domain of the ring into evenly-spaced angular patches in azimuth $\phi \in [0, 2\pi)$ with random amplitudes and phases as shown in Figure 5. We will also assume that the scatterers on this ring are located at delay τ' and write the impulse response as follows:

$$h(\tau, t; \tau') = \sum_{n=0}^{N-1} a_n(t) e^{-j\psi_n(t)} \delta(\tau - \tau') \tag{16}$$

where a_n is the real-valued amplitude of scatterer n and the phase of scatterer n is given by:

$$\psi_n(t) = 2\pi f \tau' - 2\pi \rho_n t - \zeta_n, \tag{17}$$

where f is the carrier frequency, τ and ρ_n are the delay and Doppler shift, respectively, of scatterer n, and ζ_n is a uniformly-distributed random phase over $[0, 2\pi)$. We will assume that the amplitude of each return does not change significantly over a coherent processing interval (CPI), therefore $a_n(t) \approx a_n$. We will also

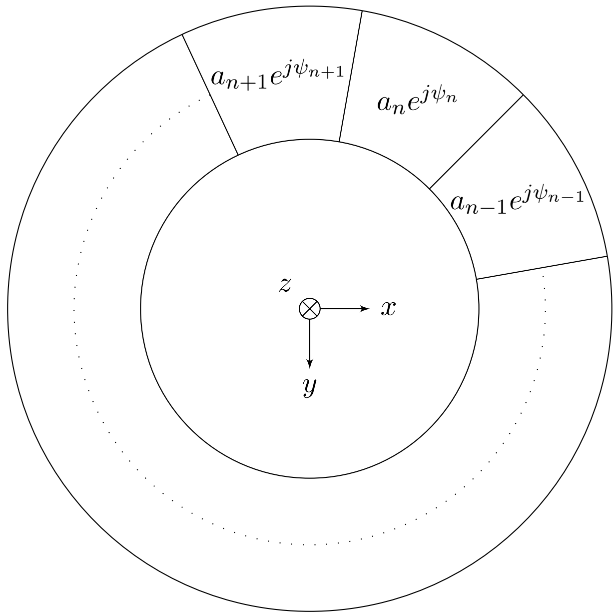

Fig. 5: Clutter patch returns for a single isorange ring.

assume that a_n and ψ_n are independent of each other. Note that because the delay τ' to each scatterer is the same and does not depend on n (which represents the azimuth angle), we can factor it out of the sum:

$$h(\tau, t; \tau') = \delta(\tau - \tau') \sum_{n=0}^{N-1} a_n e^{-j\psi_n(t)} \tag{18}$$

The autocorrelation function of the clutter signal is given by:

$$\begin{aligned} R_h(\tau_1, \tau_2, t, t+\Delta t) &= \mathbb{E}\left[h^*(\tau_1, t)\, h(\tau_2, t+\Delta t)\right] \\ &= \mathbb{E}\left[\left(\delta(\tau_1 - \tau') \sum_{n=0}^{N-1} a_n e^{j\psi_n(t)}\right)\left(\delta(\tau_2 - \tau') \sum_{m=0}^{N-1} a_m e^{-j\psi_m(t+\Delta t)}\right)\right] \\ &= \delta(\tau_1 - \tau')\delta(\tau_2 - \tau') \sum_{m=0}^{N-1}\sum_{n=0}^{N-1} \mathbb{E}\left[a_m a_n e^{-j(\psi_m(t+\Delta t) - \psi_n(t))}\right]. \end{aligned} \tag{19}$$

We will assume that the phase shifts $\{\psi_n\}$ are mutually independent, therefore:

$$
\begin{aligned}
R_h(\tau_1, \tau_2, t, t+\Delta t) &= \delta(\tau_1 - \tau')\delta(\tau_2 - \tau') \sum_{m=0}^{N-1}\sum_{n=0}^{N-1} \mathbb{E}\left[a_m a_n\right] \mathbb{E}\left[e^{-j(\psi_m(t+\Delta t) - \psi_n(t))}\right] \\
&= \delta(\tau_1 - \tau')\delta(\tau_2 - \tau') \sum_{n=0}^{N-1} \mathbb{E}\left[a_n^2\right] e^{-j(\psi_n(t+\Delta t) - \psi_n(t))} \\
&= \delta(\tau_1 - \tau')\delta(\tau_2 - \tau') \sum_{n=0}^{N-1} \mathbb{E}\left[a_n^2\right] e^{j2\pi\rho_n \Delta t} = \\
&= R_h(\tau_1, \tau_2, \Delta t; \tau')
\end{aligned} \tag{20}
$$

Note that $\mathbb{E}\left[a_n^2\right]$ is simply the channel gain from scatterer n, therefore using (4) and scaling it to account for the fact that the surface area is smaller by a factor of $1/N$, we obtain:

$$
\begin{aligned}
\mathbb{E}\left[a_n^2\right] &= \frac{1}{N}\frac{P_R}{P_T} \\
&= \frac{G^2(n\Delta\phi, \theta)\,\lambda^2}{(4\pi)^3\,(\frac{1}{2}c\tau')^4} \cdot \frac{\sigma^0}{N} \cdot \frac{\pi}{2}c^2\tau'\,d\tau'.
\end{aligned} \tag{21}
$$

Note that $N = 2\pi/\Delta\phi$, where $\Delta\phi$ is the angular spacing between patches, which upon substituting in (21) yields:

$$
\mathbb{E}\left[a_n^2\right] = \frac{\lambda^2\sigma^0 \cdot \frac{\pi}{2}c^2\tau'\,d\tau'}{(4\pi)^3\,(\frac{1}{2}c\tau')^4} \cdot \frac{1}{2\pi} G^2(n\Delta\phi, \theta)\,\Delta\phi \tag{22}
$$

Combining this with (20) and taking the limit as $N \to \infty$ yields

$$
\begin{aligned}
R_h(\tau_1, \tau_2, \Delta t; \tau') &= \delta(\tau_1 - \tau')\delta(\tau_2 - \tau') \frac{\lambda^2\sigma^0\frac{\pi}{2}c^2\tau'\,d\tau'}{(4\pi)^3\,(\frac{1}{2}c\tau')^4} \lim_{N\to\infty} \frac{1}{2\pi} \sum_{n=0}^{N-1} G^2(n\Delta\phi, \theta)\, e^{j2\pi\rho_n\Delta t}\,\Delta\phi \\
&= \delta(\tau_1 - \tau')\delta(\tau_2 - \tau') \frac{\lambda^2\sigma^0 \cdot \frac{\pi}{2}c^2\tau'\,d\tau'}{(4\pi)^3\,(\frac{1}{2}c\tau')^4} \frac{1}{2\pi} \int_{-\pi}^{\pi} G^2(\phi, \theta)\, e^{j2\pi\rho'(\phi,\theta)\Delta t}\,d\phi
\end{aligned} \tag{23}
$$

The Doppler shift of the infinitesimal scatterer located at azimuth ϕ, $\rho'(\phi)$, is given as follows:

$$
\begin{aligned}
\rho'(\phi, \theta) &= \frac{2}{\lambda}\left(v_x \cos\theta\cos\phi + v_y\cos\theta\sin\phi + v_z\sin\theta\right) \\
&= \rho_x\cos\theta\cos\phi + \rho_y\cos\theta\sin\phi + \rho_z\sin\theta
\end{aligned} \tag{24}
$$

where v_x, v_y, and v_z are the x, y, and z components of the aircraft velocity vector, respectively, and $\rho_x = 2v_x/\lambda$, $\rho_y = 2v_y/\lambda$, and $\rho_z = 2v_z/\lambda$. Note that this autocorrelation function corresponds to the return from a single isorange ring; to obtain the autocorrelation from the entire sea surface we will take

advantage of the US assumption of this channel that the return from different range increments are uncorrelated and thus that the overall autocorrelation is just the sum of the autocorrelations from each ring, implying an integral over τ':

$$R_h(\tau_1, \tau_2, \Delta t) = \int R_h(\tau_1, \tau_2, \Delta t; \tau'). \tag{25}$$

Note the omission of the differential $d\tau'$ due to it already being included in $R_h(\tau_1, \tau_2, \Delta t; \tau')$. Using the sifting property of the delta function to complete the integral yields:

$$\begin{aligned}\int R_h(\tau_1, \tau_2, \Delta t; \tau') &= \delta(\tau_1 - \tau_2) \frac{\lambda^2 \sigma^0 \cdot \frac{\pi}{2} c^2 \tau_1}{(4\pi)^3 \, (\frac{1}{2} c \tau_1)^4} \cdot \frac{1}{2\pi} \int_{-\pi}^{\pi} G^2(\phi, \theta) \, e^{j 2\pi \rho'(\phi,\theta) \Delta t} \, d\phi \\ &= \delta(\tau_1 - \tau_2) \, A_h(\tau_1, \Delta t).\end{aligned} \tag{26}$$

Note that the autocorrelation function is in the form required for a WSSUS random process and thus we can immediately identify the WSSUS correlation function $A_h(\tau, \Delta t)$ from (26):

$$\begin{aligned}A_h(\tau, \Delta t) &= \frac{\lambda^2 \sigma^0 \cdot \frac{\pi}{2} c^2 \tau}{(4\pi)^3 \, (\frac{1}{2} c \tau)^4} \cdot \frac{1}{2\pi} \int_{-\pi}^{\pi} G^2(\phi, \theta) \, e^{j 2\pi \rho'(\phi,\theta) \Delta t} \, d\phi \\ &= \frac{\lambda^2 c \, \sigma^0}{(4\pi)^3 \, (\frac{1}{2} c \tau)^3} \cdot \frac{1}{2} \int_{-\pi}^{\pi} G^2(\phi, \theta) \, e^{j 2\pi \rho'(\phi,\theta) \Delta t} \, d\phi \\ &= \frac{\lambda^2 c \, \sigma^0}{(4\pi)^3 \, (\frac{1}{2} c \tau)^3} \int_{0}^{\pi} G^2(\phi, \theta) \, e^{j 2\pi \rho'(\phi,\theta) \Delta t} \, d\phi,\end{aligned} \tag{27}$$

where the last equality is due to the fact that the integrand is an even function of ϕ. To find the scattering function C_η, we take the Fourier transform of (27) with respect to Δt:

$$\begin{aligned}C_\eta(\tau, \rho) &= \mathcal{F}_{\Delta t} \left[A_h(\tau, \Delta t) \right] \\ &= \frac{\lambda^2 c \, \sigma^0}{(4\pi)^3 \, (\frac{1}{2} c \tau)^3} \int_{0}^{\pi} G^2(\phi, \theta) \, \mathcal{F}_{\Delta t} \left[e^{j 2\pi \rho'(\phi,\theta) \Delta t} \right] \, d\phi \\ &= \frac{\lambda^2 c \, \sigma^0}{(4\pi)^3 \, (\frac{1}{2} c \tau)^3} \int_{0}^{\pi} G^2(\phi, \theta) \, \delta(\rho - \rho'(\phi, \theta)) \, d\phi\end{aligned} \tag{28}$$

The integral in (28) must be solved using a change of variable to eliminate the ϕ dependence in the argument of the delta function to allow for the evaluation of the integral. Recall that under our coordinate system definition $v_y = 0$, therefore the Doppler shift is:

$$\rho'(\phi, \theta) = \rho_x \cos\theta \cos\phi + \rho_z \sin\theta \tag{29}$$

$$\implies \quad \cos\phi = \frac{\rho' - \rho_z \sin\theta}{\rho_x \cos\theta}. \tag{30}$$

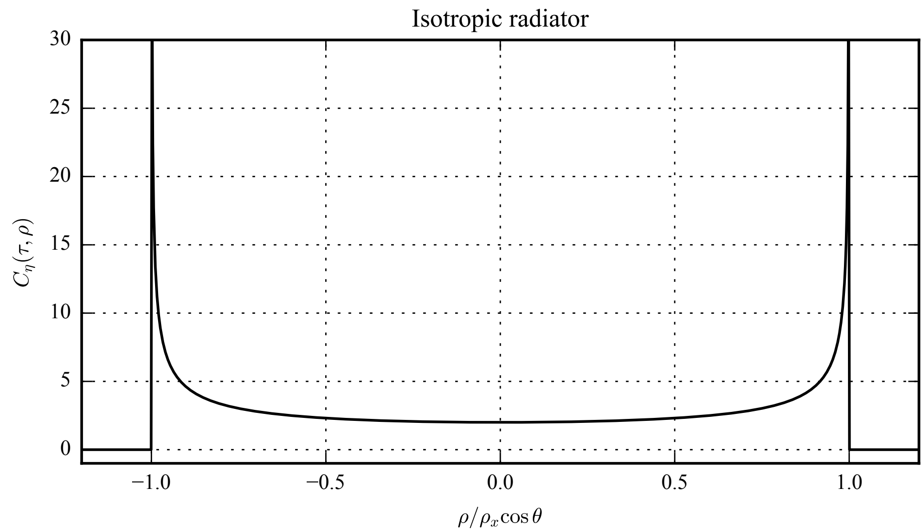

Fig. 6: Normalized Doppler spectrum for an isotropic radiator with $v_z = 0$.

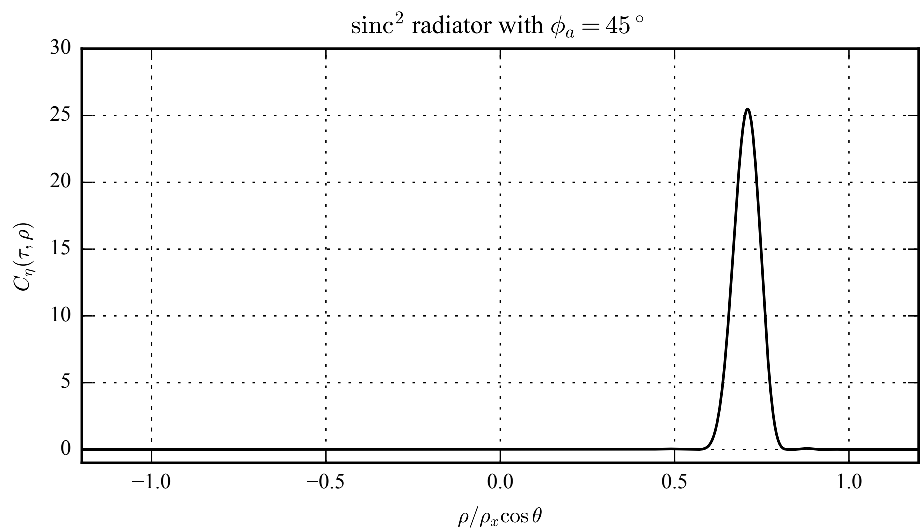

Fig. 7: Normalized Doppler spectrum for a directive radiator with $v_z = 0$.

Over the region of integration, we can solve for ϕ and perform the variable substitution:

$$\phi = \cos^{-1}\left(\frac{\rho' - \rho_z \sin\theta}{\rho_x \cos\theta}\right)$$
$$\implies d\phi = -\frac{1}{\rho_x \cos\theta}\frac{1}{\sqrt{1-\left(\frac{\rho'-\rho_z\sin\theta}{\rho_x\cos\theta}\right)^2}}d\rho = \frac{-1}{\sqrt{(\rho_x\cos\theta)^2 - (\rho' - \rho_z\sin\theta)^2}}d\rho \tag{31}$$

$$\implies \int_0^{\pi} G^2(\phi,\theta)\,\delta(\rho - \rho'(\phi,\theta))\,d\phi$$
$$= \int_{\rho_z\sin\theta-\rho_x\cos\theta}^{\rho_z\sin\theta+\rho_x\cos\theta} G^2(\phi(\rho'),\theta)\,\delta\left(\rho-\rho'\right)\,\frac{1}{\sqrt{(\rho_x\cos\theta)^2-(\rho'-\rho_z\sin\theta)^2}}\,d\rho'$$
$$= \begin{cases} \frac{G^2(\phi(\rho),\theta)}{\sqrt{(\rho_x\cos\theta)^2-(\rho-\rho_z\sin\theta)^2}}, & |\rho-\rho_z\sin\theta| < \rho_x\cos\theta \\ \\ 0, & \text{else.} \end{cases} \tag{32}$$

Combining this result with (28) yields:

$$C_\eta(\tau,\rho) = \begin{cases} \frac{\lambda^2 c}{(4\pi)^3}\cdot\frac{\sigma^0}{(\frac{1}{2}c\tau)^3}\cdot\frac{G^2(\phi(\rho),\theta)}{\sqrt{(\rho_x\cos\theta)^2-(\rho-\rho_z\sin\theta)^2}}, & |\rho-\rho_z\sin\theta| < \rho_x\cos\theta \\ \\ 0, & \text{else.} \end{cases} \tag{33}$$

Many of the factors in (33) have an implicit dependence on τ that has been suppressed for brevity– the full form is shown below:

$$C_\eta(\tau,\rho) = \begin{cases} \frac{\lambda^2 c}{(4\pi)^3}\cdot\frac{\sigma^0(\alpha(\tau))}{(\frac{1}{2}c\tau)^3}\cdot\frac{G^2(\phi(\tau,\rho),\theta(\tau))}{\sqrt{(\rho_x\cos(\theta(\tau)))^2-(\rho-\rho_z\sin(\theta(\tau)))^2}}, & |\rho-\rho_z\sin(\theta(\tau))| < \rho_x\cos(\theta(\tau)) \\ \\ 0, & \text{else.} \end{cases} \tag{34}$$

This result generalizes the Clarke model to the case when the scatterers are no longer located in the same plane as the velocity vector of the radar [40]. A plot of the normalized Doppler spectrum for a given range was generated using (32) and is plotted in Figure 6 for an isotropic radiator (i.e. $G = 1$) and for a directive radiator in Figure 7 with antenna pattern $G(\phi,\theta) = 3\,\mathrm{sinc}^2(5(\phi - \frac{\pi}{4}))$ (i.e. the antenna is pointed $45°$ counterclockwise in azimuth from the $x-$axis). It can be seen from Figure 6 that when the energy is evenly radiated in all directions the Doppler shift of the returns is focused near $\pm\rho_x\cos\theta$, the peak Doppler shift, but it can be seen from Figure 7 that the directivity of the antenna focuses the Doppler spectrum around the Doppler shift of the patch of the sea surface the beam is pointed at.

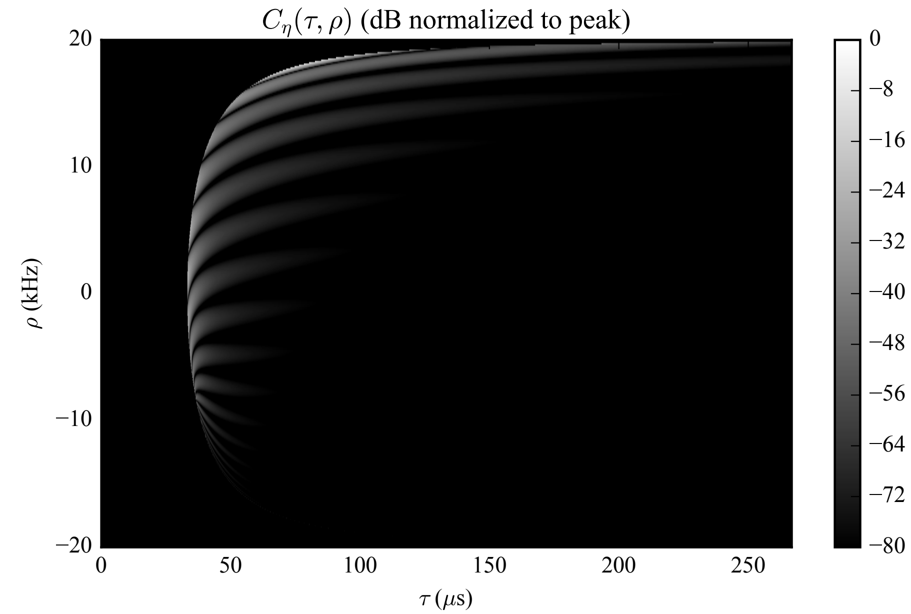

Fig. 8: Scattering function of sea clutter channel.

A plot of the scattering function over the full $\tau - \rho$ plane was generated with a circularly-symmetric sinc^2 antenna pattern generated as follows. The basic antenna pattern shape (pointed at $\phi = \theta = 0$ rad) is given by:

$$G_0(\phi,\theta) = D\,\mathrm{sinc}\left(\frac{W}{B}\sqrt{\phi^2+\theta^2}\right)^2, \tag{35}$$

where D is the directivity in linear units, B is the beamwidth in rad, $W = 0.88589$ rad is a normalization constant, and (ϕ,θ) are given in rad. Correctly rotating the antenna pattern to depression angle θ_a requires a nonlinear transformation of the angular coordinates:

$$G(\phi,\theta) = G_0(\phi'(\phi,\theta;\theta_a), \theta'(\phi,\theta;\theta_a)) \tag{36}$$

with the transformation equations given as follows:

$$\phi'(\phi,\theta;\theta_a) = \mathrm{atan2}(\cos\theta\sin\phi, \cos\theta_a\cos\theta\cos\phi + \sin\theta_a\sin\theta) \tag{37}$$

$$\theta'(\phi,\theta;\theta_a) = \mathrm{atan2}(-\sin\theta_a\cos\theta\cos\phi + \cos\theta_a\sin\theta, \sqrt{(\cos\theta_a\cos\theta\cos\phi + \sin\theta_a\sin\theta)^2 + (\cos\theta\sin\phi)^2}) \tag{38}$$

A plot of the full scattering function $C_\eta(\tau,\rho)$ is computed and plotted in Figure 8 for $f = 10$ GHz, $h = 5$ km, $\mathbf{v} = [300,0,0]^T$ m/s, $\theta_a = 25^\circ$, $B = 10^\circ = 0.17453$ rad, and $D = 100 = 20$ dB. NRCS

(σ^0) data for VV polarization at X-band as a function of grazing angle α was obtained by interpolating data points taken from Figure 7.13 from [37].

3.2 Time-Frequency Power Distribution at Channel Output

One of the goals of pulse-Doppler processing is to use Doppler filtering to isolate a target in delay-Doppler space and obtain improved detection performance [35]. We can apply the theory we have developed for WSSUS scattering channels and use the scattering function C_η to predict the time-frequency power distribution of the output signal. This presentation is essentially an updated version of the derivation given in [6].

We will first use the definition of the radar ambiguity function from [42] as our building block:

$$\chi(\tau, \rho) = \int_{-\infty}^{\infty} u(t)u^*(t+\tau)e^{j2\pi\rho t}dt, \tag{39}$$

which can be thought of as the matched filter output of a unit-energy radar pulse $u(t)$ delayed in time by τ and Doppler-shifted in frequency by ρ. Consistent with our earlier definitions, we will note that the transmitted signal $x(t)$ is expressed in terms of $u(t)$ as follows:

$$x(t) = \left(\sqrt{\int_{-\infty}^{\infty} |x(t')|^2 dt'}\right) u(t) = \sqrt{E_x}u(t) \tag{40}$$

The channel output before matched-filtering, sampled at time τ is given by:

$$r(\tau) = \int\int \eta(\tau', \rho')x(\tau - \tau')e^{j2\pi\rho'\tau}d\tau'd\rho'. \tag{41}$$

If we consider just the returns from a single Doppler shift ρ and downshift them to baseband for observation we obtain:

$$\begin{aligned} r(\tau;\rho) &= e^{-j2\pi\rho\tau}\int\int \eta(\tau', \rho')x(\tau - \tau')e^{j2\pi\rho'\tau}d\tau'd\rho' \\ &= \int\int \eta(\tau', \rho')x(\tau - \tau')e^{j2\pi(\rho'-\rho)\tau}d\tau'd\rho'. \end{aligned} \tag{42}$$

This can be thought of as the output from a Doppler filterbank filter tuned to ρ. The matched-filtered output is given by:

$$\begin{aligned} y(\tau;\rho) &= u^*(-\tau) * r(\tau;\rho) \\ &= \int\int\int \eta(\tau', \rho')x(t' - \tau')e^{j2\pi(\rho'-\rho)t'}u^*(t' - \tau)dt'd\tau'd\rho' \\ &= \sqrt{E_x}\int\int\int \eta(\tau', \rho')u(t' - \tau')e^{j2\pi(\rho'-\rho)t'}u^*(t' - \tau)dt'd\tau'd\rho'. \end{aligned} \tag{43}$$

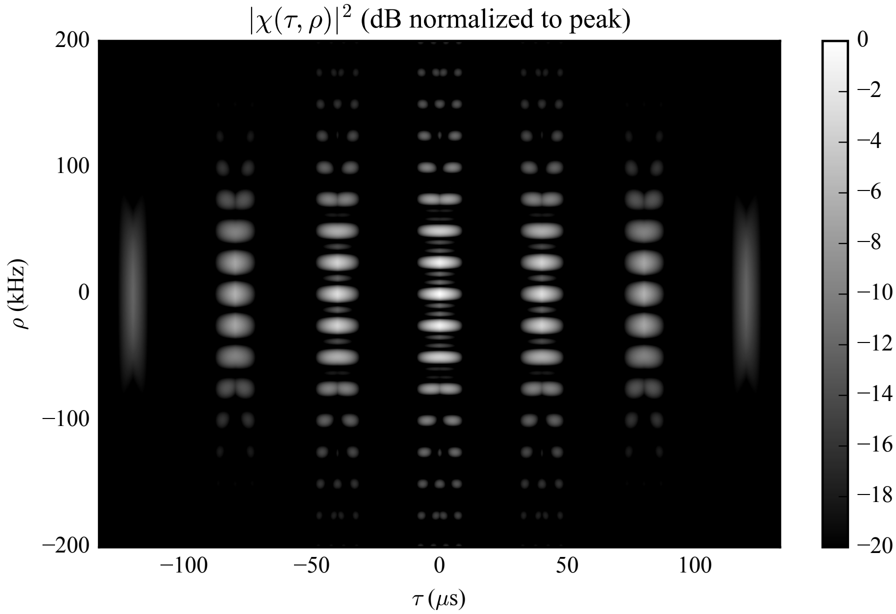

Fig. 9: Ambiguity function for a train of unmodulated rectangular pulses.

Let $t' - \tau' = \bar{t}$ and substitute this into (43), which yields:

$$\begin{aligned} y(\tau;\rho) &= \sqrt{E_x}\int\int \eta(\tau',\rho')e^{j2\pi(\rho'-\rho)\tau'}\int u(\bar{t})u^*(\bar{t}+\tau'-\tau)e^{j2\pi(\rho'-\rho)\bar{t}}d\bar{t}d\tau'd\rho' \\ &= \sqrt{E_x}\int\int \eta(\tau',\rho')e^{j2\pi(\rho'-\rho)\tau'}\chi(\tau'-\tau,\rho'-\rho)d\tau'd\rho'. \end{aligned} \tag{44}$$

The filter output of (44) is a random process due to η; to characterize the output power distribution we will take the expectation of the magnitude squared:

$$\begin{aligned} P(\tau,\rho) &= \mathbb{E}\left[|y(\tau;\rho)|^2\right] \\ = E_x\int\int\int\int &\mathbb{E}\left[\eta^*(\tau_1',\rho_1')\eta(\tau_2',\rho_2')\right]e^{-j2\pi(\rho_1'-\rho)\tau_1'}e^{j2\pi(\rho_2'-\rho)\tau_2'} \\ &\cdot\chi^*(\tau_1'-\tau,\rho_1'-\rho)\chi(\tau_2'-\tau,\rho_2'-\rho)d\tau_1'd\tau_2'd\rho_1'd\rho_2'. \end{aligned} \tag{45}$$

Using (13), we obtain:

$$\begin{aligned} P(\tau,\rho) &= E_x\int\int C_\eta(\tau',\rho')|\chi(\tau'-\tau,\rho'-\rho)|^2 d\tau'd\rho' \\ &= E_x\,C_\eta(\tau,\rho)**|\chi(-\tau,-\rho)|^2 \\ &= E_x\,C_\eta(\tau,\rho)**|\chi(\tau,\rho)|^2 \end{aligned} \tag{46}$$

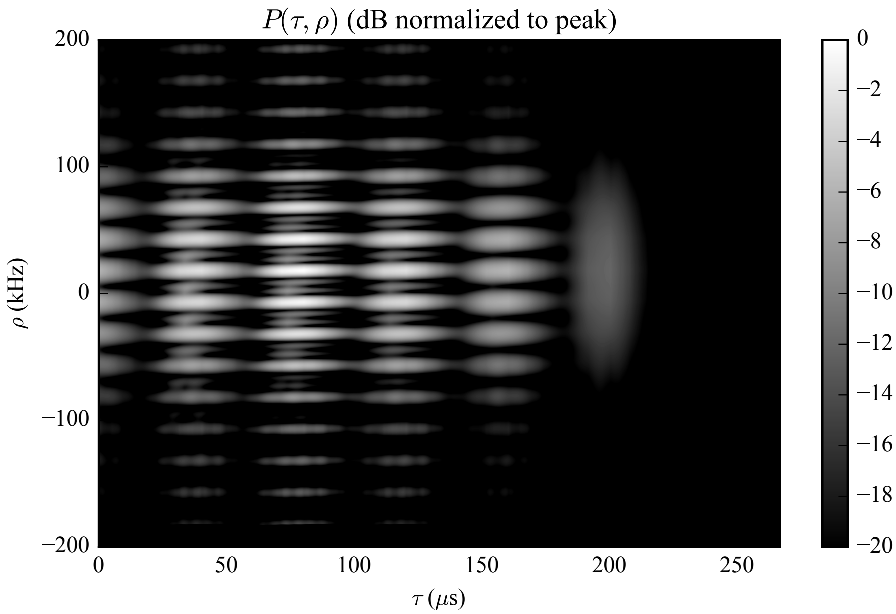

Fig. 10: Output power distribution from a sea clutter channel with an input pulse train of unmodulated rectangular pulses.

where $**$ denotes two-dimensional convolution, and the identity $|\chi(-\tau,-\rho)| = |\chi(\tau,\rho)|$ has been used to simplify the expression.

To illustrate an example scattered power distribution, we will use a train of constant-frequency rectangular pulses of duration T. The equation for a single pulse is given by:

$$u(t) = \frac{1}{\sqrt{T}} \operatorname{rect}\left(\frac{t}{T}\right), \tag{47}$$

whose ambiguity function magnitude squared is given by [42]:

$$|\chi_T(\tau,\rho)|^2 = \begin{cases} \left|\left(1 - \frac{|\tau|}{T}\right) \operatorname{sinc}\left(T\rho\left(1 - \frac{|\tau|}{T}\right)\right)\right|^2, & |\tau| \le T \\ 0, & \text{else.} \end{cases} \tag{48}$$

The ambiguity function magnitude-squared of the train of N pulses with pulse repetition interval (PRI) T_r is given by:

$$|\chi(\tau,\rho)|^2 = \begin{cases} \left| \frac{1}{N} \sum_{p=-(N-1)}^{N-1} |\chi_T(\tau - pT_r, \rho)| \left| \frac{\sin(\pi\rho(N-|p|)T_r)}{\sin(\pi\rho T_r)} \right| \right|^2, & |\tau| \leq NT_r \\ 0, & \text{else.} \end{cases} \tag{49}$$

The magnitude-squared ambiguity function of the pulse train is plotted in Figure 9 for a train with $N = 4$ pulses with pulse width $T = 10$ μs and PRI $T_r = 40$ μs.

Using equation (46) and the scattering function plotted in Figure 8 we compute the output power distribution $P(\tau,\rho)$ and plot it in Figure 10. It can be seen that the output power distribution consists of a repetition of blurred copies of the scattering function C_η.

3.3 Signal-to-Clutter Ratio

Because the output of the radar scattering channel is linear, we can use use the superposition principle of (9) to model the return from multiple objects, such as a ship in sea clutter. The scattering function for a point target with RCS σ at delay $\bar{\tau}$ and Doppler shift $\bar{\rho}$ is derived using the radar range equation:

$$C_{\eta'}(\tau,\rho) = \frac{G^2(\phi(\tau,\rho),\theta(\tau))\lambda^2\sigma}{(4\pi)^3(\frac{1}{2}c\tau)^4}\delta(\tau-\bar{\tau})\delta(\rho-\bar{\rho}), \tag{50}$$

which implies that the output power distribution is given by:

$$\begin{aligned} P'(\tau,\rho) &= E_x\, C_{\eta'}(\tau,\rho) ** |\chi(\tau,\rho)|^2 \\ &= E_x \frac{G^2(\phi(\bar{\tau},\bar{\rho}),\theta(\bar{\tau}))\lambda^2\sigma}{(4\pi)^3(\frac{1}{2}c\bar{\tau})^4} |\chi(\tau-\bar{\tau},\rho-\bar{\rho})|^2. \end{aligned} \tag{51}$$

It is clear from this result that the resolution in delay-Doppler is fundamentally limited by the resolution of the radar pulse, as manifested by the width of the ambiguity function along the τ and ρ axes.

Detection probability is usually expressed as a function of the signal-to-noise-plus-clutter ratio or just the signal-to-clutter ratio if the detection performance is clutter-limited [17]. Using (34), (46), and (51), we can now easily compute the signal-to-clutter ratio (SCR) as a function of delay and Doppler, $\gamma(\tau,\rho)$, for a

point target embedded in sea clutter:

$$\gamma(\tau,\rho) = \frac{P'(\tau,\rho)}{P(\tau,\rho)}$$

$$= \begin{cases} \dfrac{G^2(\phi(\tau,\rho),\theta(\tau))\,\sigma|\chi(\tau-\bar{\tau},\rho-\bar{\rho})|^2/\left(\frac{1}{2}c\tau\right)^4}{\left(\frac{G^2(\phi(\tau,\rho),\theta(\tau))\,c\sigma^0(\alpha(\tau))}{\left(\frac{1}{2}c\tau\right)^3\sqrt{(\rho_x\cos(\theta(\tau)))^2-(\rho-\rho_z\sin(\theta(\tau)))^2}}\right)**|\chi(\tau,\rho)|^2}, & |\rho-\rho_z\sin(\theta(\tau))| < \rho_x\cos(\theta(\tau)) \\ \infty, & \text{else.} \end{cases} \tag{52}$$

Note that in the regions of the $\tau - \rho$ plane where the clutter power is nonzero, the SCR is independent of the transmitted signal energy. This result is general enough to account for straddling loss if the spectrum is sampled at points $\tau \neq \bar{\tau}$ and $\rho \neq \bar{\rho}$ in a digital processing system.

4. CONCLUSION AND FUTURE WORK

In this work we have presented a new mathematical formulation into which the radar sea clutter modeling problem can be cast which allows for a conceptually easy way to study the time-frequency characteristics of the scattered signal. By presenting the problem in this form, the received range-Doppler map can be easily and quickly computed for an arbitrary pulse shape, antenna pattern, and NRCS angular distribution.

Future work will focus on studying the validity of the fundamental assumptions undertaken, particularly the assumption that the scattering channel can be modeled accurately by a WSSUS random process. It is hoped that the compactness of this mathematical representation will facilitate more rapid development of effective clutter mitigation techniques in the future.

ACKNOWLEDGMENTS

The authors would like to acknowledge Applied Technology, Inc. and the U.S. Naval Research Lab for supporting this work.

REFERENCES

1. A. Goldsmith, *Wireless Communications* (Cambridge University Press, 2005).
2. P. Bello, "Characterization of randomly time-variant linear channels," *IEEE Transactions on Communications Systems* **11**(4), 360–393 (December 1963), ISSN 0096-1965, doi: 10.1109/TCOM.1963.1088793.
3. J. Proakis and M. Salehi, *Digital Communications* (McGraw-Hill, 5th edition, 2008).
4. G. Matz, H. Bolcskei, and F. Hlawatsch, "Time-frequency foundations of communications: Concepts and tools," *IEEE Signal Processing Magazine* **30**(6), 87–96 (Nov 2013), ISSN 1053-5888, doi: 10.1109/MSP.2013.2269702.
5. R. Price and P. E. Green, Jr., "Signal processing in radar astronomy– communication via fluctuating multipath media," rept. 234, MIT Lincoln Laboratory (October 1960).
6. P. E. Green, Jr., "Radar astronomy measurement techniques," rept. 282, MIT Lincoln Laboratory (December 1962).
7. H. L. Van Trees, *Detection, Estimation, and Modulation Theory*, volume 3 (John Wiley & Sons, 1971).
8. S. M. Kay and S. B. Doyle, "Rapid estimation of the range-doppler scattering function," *IEEE Transactions on Signal Processing* **51**(1), 255–268 (Jan 2003), ISSN 1053-587X, doi: 10.1109/TSP.2002.806579.
9. N. Gaarder, "Scattering function estimation," *IEEE Transactions on Information Theory* **14**(5), 684–693 (Sep 1968), ISSN 0018-9448, doi: 10.1109/TIT.1968.1054194.
10. L.-T. Nguyen, B. Senadji, and B. Boashash, "Scattering function and time-frequency signal processing," in *2001 IEEE International Conference on Acoustics, Speech, and Signal Processing. Proceedings (Cat. No.01CH37221)*, volume 6, pp. 3597–3600 vol.6 (2001), doi: 10.1109/ICASSP.2001.940620.
11. J. K. Harmon, "Planetary delay-doppler radar and the long-code method," *IEEE Transactions on Geoscience and Remote Sensing* **40**(9), 1904–1916 (Sep 2002), ISSN 0196-2892, doi: 10.1109/TGRS.2002.803731.
12. O. Oktay, G. E. Pfander, and P. Zheltov, "Reconstruction of the scattering function of overspread radar targets," *IET Signal Processing* **8**(9), 1018–1024 (2014), ISSN 1751-9675, doi: 10.1049/iet-spr.2013.0304.
13. G. E. Pfander and P. Zheltov, "Sampling of stochastic operators," *IEEE Transactions on Information Theory* **60**(4), 2359–2372 (April 2014), ISSN 0018-9448, doi: 10.1109/TIT.2014.2301444.
14. G. E. Pfander and P. Zheltov, "Estimation of overspread scattering functions," *IEEE Transactions on Signal Processing* **63**(10), 2451–2463 (May 2015), ISSN 1053-587X, doi: 10.1109/TSP.2015.2403309.
15. B. Boashash, *Time-Frequency Signal Analysis and Processing: A Comprehensive Reference* (Academic Press, 2016).

16. S. P. Sira, D. Cochran, A. Papandreou-Suppappola, D. Morrell, W. Moran, S. D. Howard, and R. Calderbank, "Adaptive waveform design for improved detection of low-RCS targets in heavy sea clutter," *IEEE Journal of Selected Topics in Signal Processing* **1**(1), 56–66 (June 2007), ISSN 1932-4553, doi: 10.1109/JSTSP.2007.897048.

17. M. A. Richards, *Fundamentals of Radar Signal Processing* (IET/McGraw-Hill Education, 2nd edition, 2014).

18. D. E. Kerr and H. Goldstein, "Radar targets and echoes," in *Propagation of Short Radio Waves*, volume 13, chapter 6 (McGraw-Hill, 1951).

19. A. H. Schooley, "Some limiting cases of radar sea clutter noise," *Proceedings of the IRE* **44**(8), 1043–1047 (Aug 1956), ISSN 0096-8390, doi: 10.1109/JRPROC.1956.275048.

20. M. Katzin, "On the mechanisms of radar sea clutter," *Proceedings of the IRE* **45**(1), 44–54 (Jan 1957), ISSN 0096-8390, doi: 10.1109/JRPROC.1957.278255.

21. S. O. Rice, "Reflection of electromagnetic waves from slightly rough surfaces," *Communications on pure and applied mathematics* **4**(2-3), 351–378 (1951).

22. J. DeLorenzo and E. Cassedy, "A study of the mechanism of sea surface scattering," *IEEE Transactions on Antennas and Propagation* **14**(5), 611–620 (Sep 1966), ISSN 0018-926X, doi: 10.1109/TAP.1966.1138737.

23. D. K. Barton, *Radars: Radar Clutter*, volume 5 (Artech House, 1974).

24. J. Wang and X. Xu, "Simulation of correlated low-grazing-angle sea clutter based on phase retrieval," *IEEE Transactions on Geoscience and Remote Sensing* **53**(7), 3917–3930 (July 2015), ISSN 0196-2892, doi: 10.1109/TGRS.2014.2388211.

25. K. Ward, *Sea Clutter: Scattering, the K Distribution and Radar Performance*, Radar, Sonar &; Navigation (Institution of Engineering and Technology, 2013), URL `http://digital-library.theiet.org/content/books/ra/pbra025e`.

26. E. Jakeman and P. N. Pusey, "The statistics of light scattered by a random phase screen," *Journal of Physics A: Mathematical, Nuclear and General* **6**(7), L88 (1973), URL `http://stacks.iop.org/0301-0015/6/i=7/a=004`.

27. E. Jakeman and P. N. Pusey, "Non-Gaussian fluctuations in electromagnetic radiation scattered by random phase screen I: Theory," *Journal of Physics A: Mathematical and General* **8**(3), 369 (1975), URL `http://stacks.iop.org/0305-4470/8/i=3/a=010`.

28. P. N. Pusey and E. Jakeman, "Non-Gaussian fluctuations in electromagnetic radiation scattered by a random phase screen II: Application to dynamic scattering in liquid crystal," *Journal of Physics A: Mathematical and General* **8**(3), 392 (1975), URL `http://stacks.iop.org/0305-4470/8/i=3/a=011`.

29. E. Jakeman and P. Pusey, "A model for non-Rayleigh sea echo," *IEEE Transactions on Antennas and Propagation* **24**(6), 806–814 (Nov 1976), ISSN 0018-926X, doi: 10.1109/TAP.1976.1141451.

30. K. D. Ward, "Compound representation of high resolution sea clutter," *Electronics Letters* **17**(16), 561–563 (August 1981), ISSN 0013-5194, doi: 10.1049/el:19810394.

31. S. Watts and K. D. Ward, "Spatial correlation in K-distributed sea clutter," *Communications, Radar and Signal Processing, IEE Proceedings F* **134**(6), 526–532 (October 1987), ISSN 0143-7070, doi: 10.1049/ip-f-1.1987.0090.

32. K. D. Ward, R. J. A. Tough, and P. W. Shepherd, "Modelling sea clutter: correlation, resolution and non-Gaussian statistics," in *Radar 97 (Conf. Publ. No. 449)*, pp. 95–99 (Oct 1997), doi: 10.1049/cp:19971639.

33. F. J. Ryan, "User's guide for the VTRPE tropospheric/ionospheric electromagnetic propagation model, version 3.x (version O)," rept., Maritime Surveillance Division, Space and Naval Warfare Systems Center, San Diego (July 2005).

34. R. H. Ott, "A line-of-sight propagation model for calculating atmospheric, sea, terrain multipath, and clutter at microwave frequencies," *Radio Science* **32**(2), 369–386 (1997), ISSN 1944-799X, doi: 10.1029/96RS03199, URL `http://dx.doi.org/10.1029/96RS03199`.

35. G. W. Stimson, *Introduction to Airborne Radar* (SciTech Publishing, 1998).

36. E. Westerfield, R. Prager, and J. Stewart, "Processing gains against reverberation (clutter) using matched filters," *IRE Transactions on Information Theory* **6**(3), 342–348 (June 1960), ISSN 0096-1000, doi: 10.1109/TIT.1960.1057573.

37. M. I. Skolnik, *Introduction to Radar Systems* (McGraw-Hill, 3rd edition, 2001).

38. H. Ding, J. Guan, N. Liu, and G. Wang, "New spatial correlation models for sea clutter," *IEEE Geoscience and Remote Sensing Letters* **12**(9), 1833–1837 (Sept 2015), ISSN 1545-598X, doi: 10.1109/LGRS.2015.2430371.

39. G. Matz, "On non-WSSUS wireless fading channels," *IEEE Transactions on Wireless Communications* **4**(5), 2465–2478 (Sept 2005), ISSN 1536-1276, doi: 10.1109/TWC.2005.853905.

40. R. H. Clarke, "A statistical theory of mobile-radio reception," *The Bell System Technical Journal* **47**(6), 957–1000 (July 1968), ISSN 0005-8580, doi: 10.1002/j.1538-7305.1968.tb00069.x.

41. T. Feng and T. R. Field, "Statistical analysis of mobile radio reception: an extension of Clarke's model," *IEEE Transactions on Communications* **56**(12), 2007–2012 (December 2008), ISSN 0090-6778, doi: 10.1109/TCOMM.2008.060596.

42. N. Levanon and E. Mozeson, *Radar Signals* (IEEE Press/Wiley-Interscience, 2004).